Chemical Engineering Journal 100 (2004) 95–107

Chemical Engineering Journal

www.elsevier.com/locate/cej

Unsteady temperature fields of monoliths in catalytic converters

Shi-Jin Shuai*, Jian-Xin Wang

State Key Laboratory of Automotive Safety and Energy, Tsinghua University, Beijing 100084, China

Received 22 August 2003; accepted 7 January 2004

Abstract

This paper measured unsteady temperature fields of uncoated-monolith and catalytic monolith under real engine operating conditions using thermocouples. A multi-dimensional flow model of the turbulence, heat and mass transfer, and chemical reactions in monoliths was established and numerically solved in the whole flow field of the catalytic converter. The purpose of this paper is to study unsteady warm-up characteristics of the monoliths and to investigate effects of inlet cone structure on temperature distribution of the catalytic converter. Experimental results show that the warm-up behaviors between uncoated-monolith and catalytic monolith are quite different. Simulation results indicate that the established model can qualitatively predict the warm-up characteristics. Increasing the inlet cone angle can improve the light-off characteristics of the catalysts due to high flow velocity and high temperature in the center of the monoliths.

Keywords: Catalytic converter; Temperature field; Measurement; Modeling; Optimum design

1. Introduction

Catalytic converters are being widely used in automobile industry and have already been proved to be the most effective technical solution to reduce harmful emissions from SI engines. A worldwide demand for environmental protection has enforced more stringent emission legislations. According to existing experiences in the world [1], the main emission control technology for gasoline vehicles which can meet future severe emission standards like Euro IV is still the three-way catalytic converter (TWC) plus electronic fuel injection (EFI) system. But the match of TWC with EFI and the optimum design of the catalytic converter exhaust system should be more carefully refined. The main challenge is how to reduce the hydrocarbon (HC) emitted from vehicles during the cold start. According to vehicle driving cycle tests, approximately 80% of HC is emitted in the cold start phase due to a low temperature of the exhaust gas and monolith [2]. Therefore, how to increase HC conversion efficiency during the cold start is the key to satisfy the stringent regulations, and the temperature inside the monolith is the most important parameter to decrease the HC emission. Previous studies [4,5] mainly focus on the modeling of thermal and chemical behavior of the monolith, few of them on the measurement of the temperature fields. In this paper, two-dimensional transient temperature fields of the monoliths were measured by thermocouples and simulated by computational fluid dynamics (CFD) code to study temperature distributions and warm-up characteristics of the catalytic converter.

2. Measurement of temperature in monolith

2.1. Experimental equipment

A schematic of test rig and the installation of thermocouples in the catalytic converter are shown in Figs. 1 and 2, respectively. The test engine is BN492 SI engine with a single port injection (SPI) system. The catalytic monolith is a three-way catalyst monolith, and the uncoated-monolith is made of cordierite ($2MgO{\cdot}2Al_2O_3{\cdot}5SiO_2$), with a porosity of 300 cpsi. The diameter of NiCr–NiSi thermocouples used in the experiment is 1 mm. From the rear end of the monoliths, the thermocouples are inserted into the channels at different positions along radial and axial directions (see also Fig. 3). The inlets of the test channels are sealed by temperature-resisting cement for measuring the temperature inside the monoliths. Several thermocouples protrude their heads 10 mm out of the channels for measuring the inflow gas temperature, as shown in Fig. 2. Exhaust gas from the engine has two routine lines (symbols 1 and 2 as shown in Fig. 1) leading to the catalytic converter, one is to pass

* Corresponding author. Tel.: +86-10-627-72515; fax: +86-10-627-88607.
E-mail address: sjshuai@tsinghua.edu.cn (S.-J. Shuai).

1385-8947/$ – see front matter © 2004 Elsevier B.V. All rights reserved.
doi:10.1016/j.cej.2004.01.013

Nomenclature

a_c	catalyst area per unit reactor volume (m^2 Pt/m^3)
a_v	ratio of monolith surface to monolith volume (m^2/m^3)
c_{gi}	mole fraction of species i (mol/mol)
c_{ps}	monolith specific heat (J/kg K)
c_{si}	mole fraction of species i on the surface of the monolith (mol/mol)
C_{pg}	gas specific heat capacity (J/kg K)
d	hydraulic diameter of monolith channels (m)
G	monolith orthotropic conductivity factor
h_g	gas enthalpy (J/kg)
H	gas heat transfer coefficient (W/m^2 K)
ΔH_i	reaction heat of species i (J/mol)
k_s	monolith thermal conductivity (W/m K)
K_{mi}	mass transfer coefficient of species i (m/s)
L	monolith length (mm)
M_i	molecular mass of species i (kg/kmol)
p	gas pressure (N/m^2)
R	monolith radius (mm)
R_i	chemical reaction rate of species i (mol/m^2 Pt s)
T_g	gas temperature (K)
T_s	monolith temperature (K)
U	gas velocity (m/s)
x, y, z	coordinate axes

Greek letters

α	monolith porosity
ε	dissipation rate (m^2/s^3)
κ	turbulent kinetic energy (m^2/s^2)
ρ_g	gas density (kg/m^3)
ρ_s	monolith density (kg/m^3)
υ	gas kinematic viscosity (m^2/s)

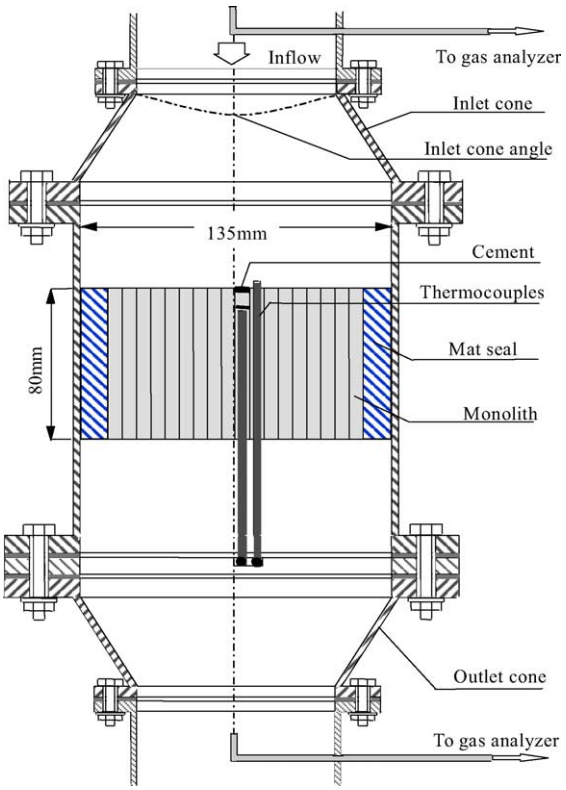

Fig. 2. Installation of thermocouples in converter.

through the heat exchanger, another is to enter the converter directly. The heat exchanger installed in routine 1 is used to cool the hot exhaust gas to a fixed temperature for an initial test temperature, which is greatly lower than the light-off temperature of the catalyst. The control valve turns the exhaust gas from routines 1 to 2 when the measurement begins.

2.2. Arrangement of measuring points

The measuring points of the thermocouples in axisymmetric planes of uncoated-monolith and catalytic monolith are

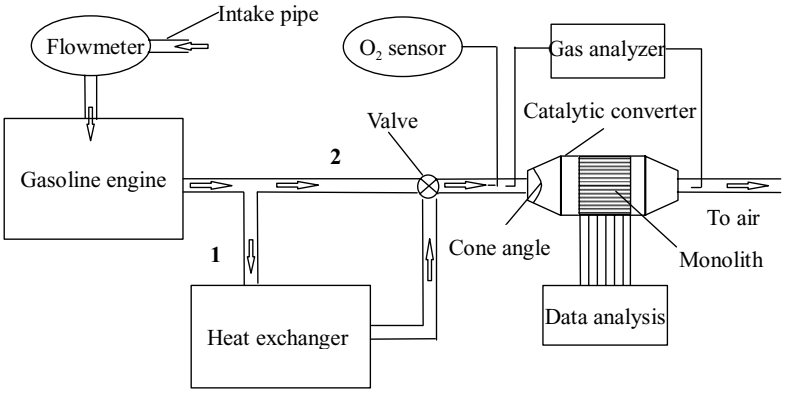

Fig. 1. Schematic of test rig.

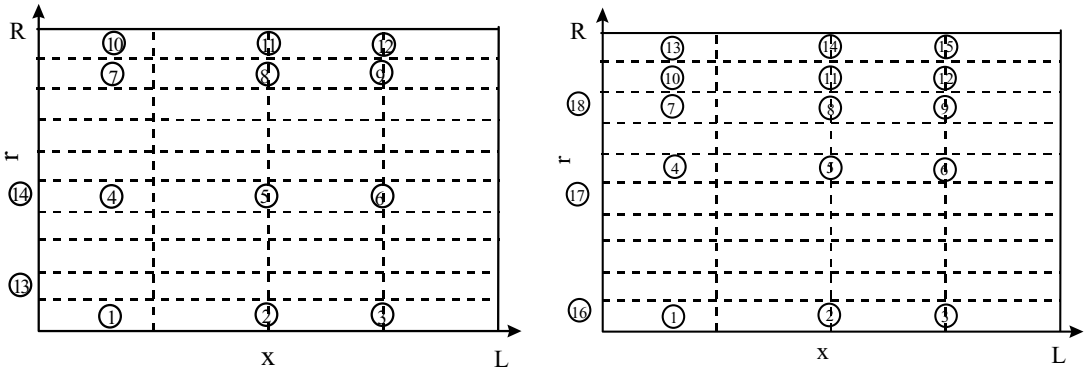

Fig. 3. Arrangement of measuring points.

arranged as shown in Fig. 3(a) and (b), respectively. Here, $r = 0$ corresponds with the centerline and $x = 0$ corresponds with the inlet of the monolith. The points are mainly distributed in the center and near the edge of the monoliths. Along axial direction, the thermocouples are located at three cross-sections with x coordinates of $0.15L$, $0.5L$ and $0.75L$ for two monoliths. The third section ($x = 0.75L$) was tried to move backward to the rear end of the monoliths as soon as possible, but the installation of the thermocouples was found to be too difficult. Along radial direction, they are located at the positions with r coordinates of $0.1R$, $0.5R$, $0.9R$ and $1R$ for uncoated-monolith, and $0.1R$, $0.6R$, $0.8R$, $0.9R$ and $1R$ for catalytic monolith. In order to obtain the gas temperatures into the monoliths, three points with r coordinates of $0.1R$, $0.5R$ and $0.8R$ are chosen for uncoated-monolith, and two points with r coordinates of $0.1R$ and $0.5R$ for catalytic monolith. The catalytic monolith will cause a larger temperature difference within the monolith due to chemical reactions. Therefore more measuring points are inserted near the edge of the monolith. The catalytic monolith has 15 measuring points, more than the uncoated-monolith.

2.3. Test results and analysis

2.3.1. Warm-up characteristics of uncoated-monolith

Researches on warm-up characteristics of uncoated-monolith can help us to understand the effect of the monolith itself on light-off performance of the catalyst. The catalytic converter used in this experiment has an inlet cone angle of 40°. The engine running conditions are as follows: engine speed is 2000 rpm; air/fuel ratio (A/F) is controlled near stoichiometric ratio; mass flow in the catalytic converter is 33.3 g/s. Before measuring, the exhaust gas passes through routine 1 pipe (see also Fig. 1) and is cooled by the heat exchanger and then goes into the catalytic converter. In this case, the inlet gas temperature is controlled at about 423 K. When the engine runs steadily, the valve is rapidly turned to routine 2 to let the exhaust gas enter the converter directly. At the same time, the temperature rising process at different time is recorded using data sampling and analyzing system.

Fig. 4(a)–(f) shows temperature contour changes in uncoated-monolith. These contours illustrate the distribution and development of the temperature field in the monolith at $x = 0.15$–$0.75L$ along axial direction and $r = 0.1$–$1R$ along radial direction. The front center of the monolith has a highest temperature due to a high flow velocity in the center of the monolith [3]. As time goes on, the high temperature field expands to the surrounding area and also moves backward with the heat flux transfer along axial and radial directions. And the temperature gradient decreases gradually and the temperature tends to be more and more uniform. Fig. 4(e) and (f) is temperature contours at 60 and 90 s, respectively. From the two figures we can see that the temperature difference between the two moments is not obvious, which indicates that the temperature in uncoated-monolith tends to be stable after 60 s. But the temperature in the edge of the monolith is still lower than that in the center because of the heat exchange with circumference near the edge.

2.3.2. Warm-up characteristics of catalytic monolith

For catalytic monolith, not only is there a convective heat transfer between the monolith and the exhaust gas, but also a large amount of heat released from the chemical reactions on the surface of the monolith. Consequently, the unsteady temperature field of catalytic monolith is quite different from uncoated-monolith. Here, all the engine test conditions and measuring process are the same as mentioned above in uncoated-monolith. But for real engines, the inlet exhaust conditions of two monoliths were found to be difficult to be controlled the same. The starting temperature (about 520 K) of the coated-monolith is higher than that (about 420 K) of the uncoated-monolith.

Fig. 5 shows the warm-up behaviors of measuring points 1 and 16, which gives the temperature of the front center of the monolith and the temperature of the exhaust gas into the monolith, respectively, as shown in Fig. 3. The figure indicates that the temperature of the monolith (point 1) is

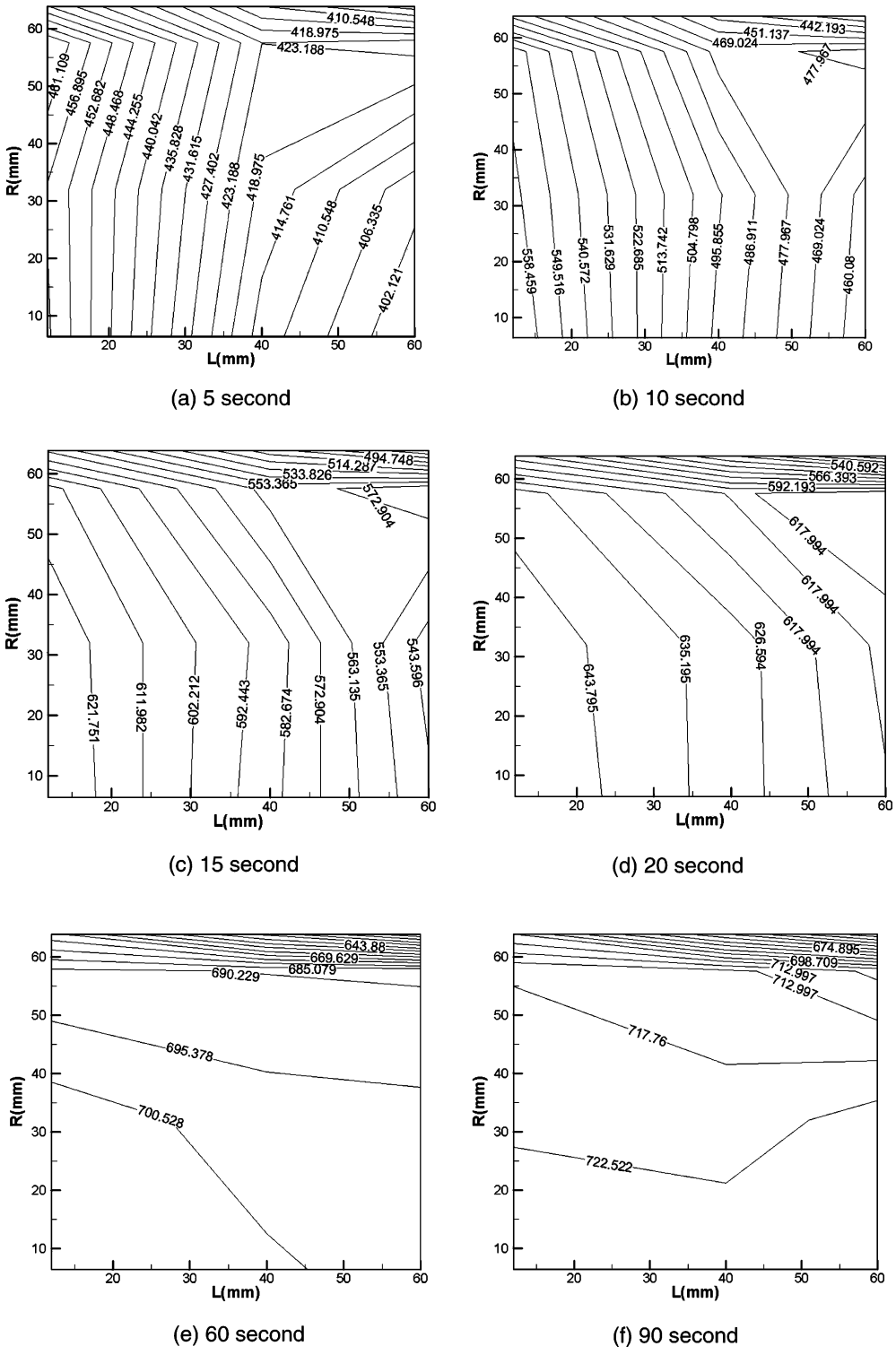

Fig. 4. Temperature contours in uncoated-monolith at different time.

lower than that of the exhaust gas (point 16, which is located just before the front end of the monolith) at the beginning of the warm-up. But after about 12 s, the temperature of point 1 begins to exceed the temperature of point 16, which means that the catalyst is activated and the released heat is now heating the monolith.

Fig. 6(a)–(f) is temperature contours in catalytic monolith at different time. Compared with Fig. 4, it is found that the development trend of unsteady temperature fields of catalytic monolith is similar to uncoated-monolith at the beginning (before the catalyst is activated), that is to say, the front center of the monolith has the highest temperature and then

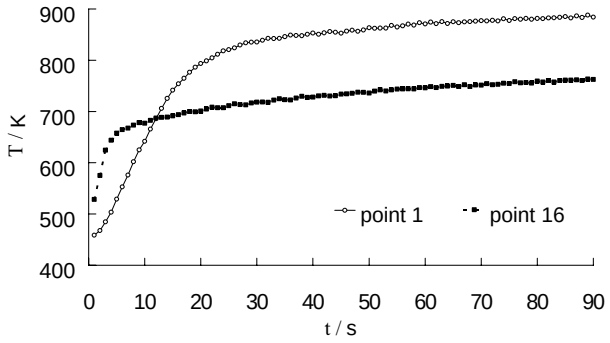

Fig. 5. Warm-up behaviors at points 1 and 16.

the high temperature field expands and moves backwards as time goes on. This is because the monolith is mainly heated by the exhaust gas during this period, and its temperature increases slowly. After the catalyst is activated, the heat from chemical reactions results in a quick rise of the temperature in the front part. As a result, the development of temperature field in catalytic monolith is quite different from that in uncoated-monolith.

From Fig. 6(e) and (f) it can be seen that at 60 s the temperature in the rear center of the monolith is close to the front part; but at 90 s the temperature in the rear center is higher than that in the front part. The main reason is that after the catalyst is activated, the monolith temperature in the front part is greatly higher than the exhaust gas. At this time the exhaust gas actually cools the monolith, so not only is the chemical reaction heat brought away by the exhaust gas, but also the growth rate of the temperature in the front part is lowered by the convective heat transfer. However, temperatures of the middle and the rear part are a little lower at the beginning, then the hot exhaust gas and released chemical reaction heat from the upstream accelerate chemical reactions downstream.

Therefore, a high temperature field appears in the middle and rear part of the monolith.

The contours also indicate that the temperature gradient on the whole monolith is very small at 5 s, the difference between the highest temperature and the lowest one is about 70 K. After the catalyst is activated, the difference grows quickly due to the heat from the chemical reactions in the monolith, for example, the difference at 10 s is about 140 K and at 15 s it is up to about 185 K; 20 s later, the difference begins to decrease and tends to be constant about 70 K as time goes on.

3. Numerical simulation of the catalytic converters

With the rapid development of CFD technology in past decades, people can utilize numerical simulation method to study the catalytic converter performance [4]. This paper uses a CFD code to simulate the transient temperature fields of the catalytic converter and investigates the effect of inlet cone structure on temperature distribution and warm-up characteristics in monoliths.

3.1. Models of flow, heat and mass transfer, chemical reactions in monoliths

A two-dimensional computational region of the axis-symmetric catalytic converter (also see Fig. 2) is divided into a free stream region and a monolith region as shown in Fig. 7. The monolith region can also be subdivided into a fluid region and a corresponding solid region. This paper considers the heat and mass transfer, chemical reactions of gaseous components at the monolith surface, and also the heat conduction in the monolith.

3.1.1. Flow governing equations

For the fluid dynamics that occur in the free stream region the Reynolds averaged Navier–Stockes equations are solved, where the standard $\kappa-\varepsilon$ turbulence model is used to close the equations. In the monolith fluid region an equivalent continuum approach [5], which views the monolith as a porous medium through which the unidirectional gas continually passes, is utilized to establish the models.

The gas flow in parallel channels of the monolith can be regarded as a fully developed laminar flow whose governing equation is given by Hagen–Poiseulle equation to calculate the pressure loss through the monolith as follows:

$$\frac{\partial p}{\partial x} = \frac{-32\upsilon\rho_g U}{\alpha d^2} \tag{1}$$

where p is the gas pressure, U the gas velocity, ρ_g the gas density, α the monolith porosity, d the hydraulic diameter of monolith channels. The gas viscosity υ which is a function of gas temperature T_g is given by [6]

$$\upsilon = (6.542\times10^{-11}T_g^2) + (6.108\times10^{-8}T_g) - 0.89\times10^{-5} \tag{2}$$

3.1.2. Heat and mass transfer equations

(1) Gas enthalpy conservation equation

$$\frac{\partial(\rho_g h_g)}{\partial t} + \frac{\partial}{\partial x}(\rho_g U h_g) = Ha_v(T_s - T_g) \tag{3}$$

where H is the gas heat transfer coefficient with a constant value; a_v the ratio of monolith surface to monolith volume; T_s the monolith temperature and the gas temperature T_g is obtained by

$$T_g = \frac{h_g}{C_{pg}} \tag{4}$$

where h_g is the gas enthalpy and C_{pg} is the gas specific heat capacity.

(2) Chemical species conservation equation

$$\frac{\partial\rho_g c_{gi}}{\partial t} + \frac{\partial}{\partial x}(\rho_g U c_{gi}) = \rho_g K_{mi} a_v (c_{si} - c_{gi}) \tag{5}$$

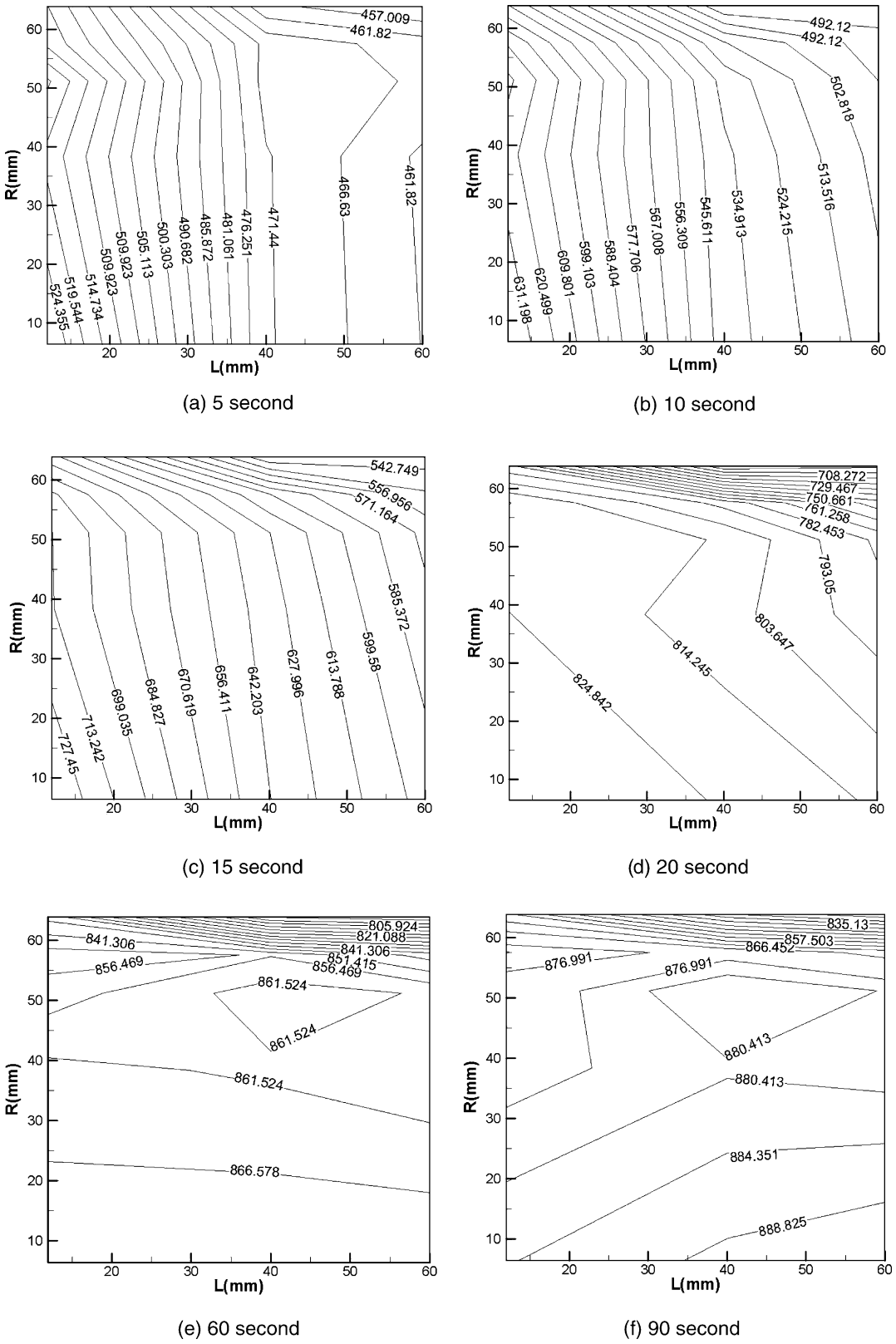

Fig. 6. Temperature contours in catalytic monolith at different time.

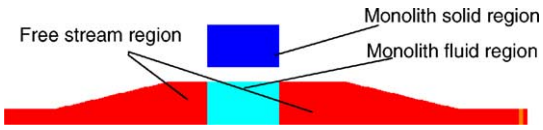

Fig. 7. Computational region of the catalytic converter.

where c_{gi} is the mole fraction of species i in the gas and c_{si} is the mole fraction of species i on the surface of the monolith; K_{mi} is the mass transfer coefficient of species i with a constant value. The concentrations of the species on the catalyst surface are governed by expressions of the form:

$$\rho_g K_{mi} a_v (c_{gi} - c_{si}) = a_c \frac{M_i R_i}{10^3} \tag{6}$$

where M_i is the molecular mass of species i; a_c the catalyst area per unit reactor volume; R_i the chemical reaction rate of species i. The term on the left side of Eq. (6) represents the diffusion process of species to and from the monolith surface. The term on the right side indicates the removal of species by the reaction.

(3) Monolith heat conduction equation

The equation governing the monolith temperature T_s behavior is essentially that of heat conduction in the monolith. Considering the orthotropic nature of the heat conduction, the governing equation takes the form:

$$(1-\alpha)c_{ps}\rho_s \frac{\partial T_s}{\partial t} - k_s \left[(1-\alpha)\frac{\partial^2 T_s}{\partial x^2} + G\left(\frac{\partial^2 T_s}{\partial y^2} + \frac{\partial^2 T_s}{\partial z^2} \right) \right] = s_1 + s_2 \tag{7}$$

where x is the gas flow direction; y and z are another two coordinate directions perpendicular to x direction; ρ_s is the monolith density; c_{ps} is the monolith specific heat capacity; k_s is the monolith thermal conductivity; G is defined as k_{eff}/k_s, where k_{eff} is the effective thermal conductivity of the composite of exhaust gas and substrate in the direction of y and z. Normally k_s and G will be dependent on the gas composition, temperature and velocity. But for simplicity both are assumed to be constant throughout the monolith. The two source items s_1 and s_2, are given by

$$s_1 = H a_v (T_g - T_s) \tag{8}$$

$$s_2 = \sum a_c R_i \Delta H_i \tag{9}$$

where s_1 is the heat transfer between the monolith and the gas; s_2 the heat released from chemical reactions; ΔH_i is the reaction heat of species i.

3.1.3. Chemical reaction equations

The chemical reactions of the catalysts on the monolith surface are very complex. This paper only considers the oxidation reactions of CO and C_3H_6 over Pt on the surface as a preliminary investigation. Propylene (C_3H_6) is assumed to be a representative of "fast oxidizing hydrocarbons". The specific reaction rate expressions (i.e., rates per unit Pt surface area) for the oxidation reactions of CO and C_3H_6 were obtained from Voltz et al. The simplified chemical reactions can be expressed by

$$CO + 0.5O_2 \rightarrow CO_2 \tag{10}$$

$$C_3H_6 + 4.5O_2 \rightarrow 3CO_2 + 3H_2O \tag{11}$$

and the reaction rates are given by

$$R_{CO} = \frac{k_1 c_{CO} c_{O_2}}{D(T_s, c)} \tag{12}$$

$$R_{C_3H_6} = \frac{k_2 c_{C_3H_6} c_{O_2}}{D(T_s, c)} \tag{13}$$

where

$$D(T_s, c) = T_s(1 + K_1 c_{CO} + K_2 c_{C_3H_6})^2 (1 + K_3 c_{CO}^2 c_{C_3H_6}^2) \times (1 + K_4 c_{NO}^{0.7}) \tag{14}$$

$$k_1 = 6.699 \times 10^9 \exp\left(\frac{-12\,556}{T_s}\right) \tag{15}$$

$$k_2 = 1.392 \times 10^{11} \exp\left(\frac{-14\,556}{T_s}\right) \tag{16}$$

$$K_1 = 65.5 \times \exp\left(\frac{961}{T_s}\right) \tag{17}$$

$$K_2 = 2.08 \times 10^3 \exp\left(\frac{361}{T_s}\right) \tag{18}$$

$$K_3 = 3.98 \times \exp\left(\frac{11\,611}{T_s}\right) \tag{19}$$

$$K_4 = 4.79 \times 10^5 \exp\left(\frac{-3733}{T_s}\right) \tag{20}$$

From the stoichiometry the reaction rate for oxygen must satisfy the following relation:

$$R_{O_2} = 0.5 R_{CO} + 4.5 R_{C_3H_6} \tag{21}$$

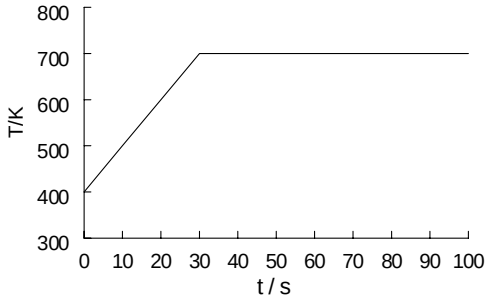

Fig. 8. Inlet temperature vs. time.

3.2. Solution conditions

In CFD, there are two basic algorithms to solve the N–S equations: one is pressure implicit splitting of operators (PISO) [7] for time dependent flows; another is semi-implicit method for pressure linked equations (SIMPLE) for steady state problems. Here we choose PISO algorithm to solve the above governing equations for the transient flows. The PISO algorithm has four steps as follows.

- Step 1: guess p, flux (use values from the previous timestep).
- Step 2: use equation to find velocity components.
- Step 3: solve the pressure equation for p.
- Step 4: correct the flux to satisfy continuity.

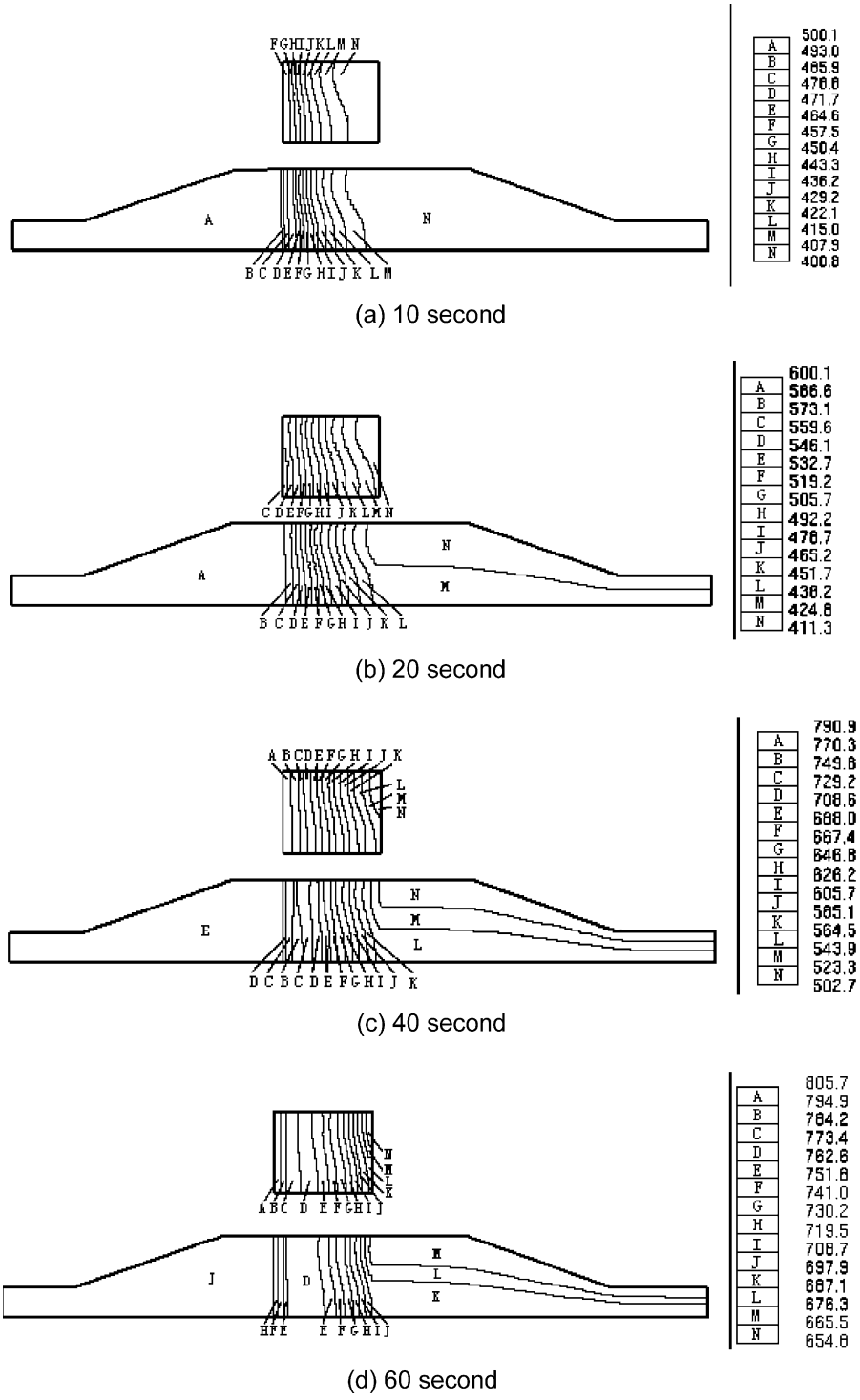

Fig. 9. Temperature contours of 40° catalytic converter at different time (K).

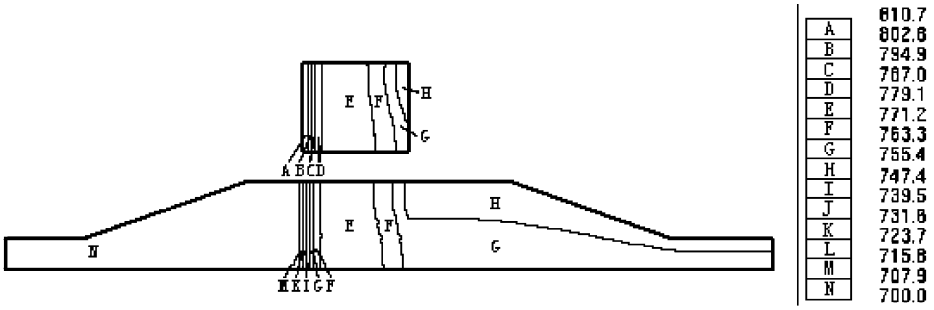

(e) 80 second

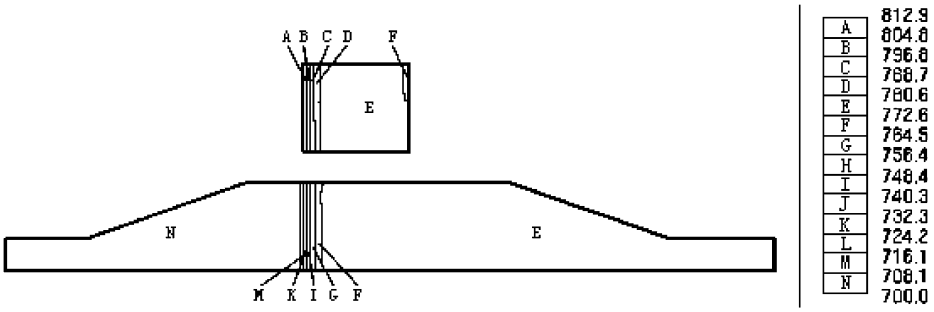

(f) 100 second

Fig. 9. (*Continued*).

Steps 3 and 4 can be iterated if necessary. This advances the solution one timestep—the whole procedure is then repeated from steps 1 to 4 for the next timestep.

Subroutines for heat and mass transfer and chemical reactions on the monolith surface are programmed by authors and solved coupling with the flow governing equations in free stream region (see also Fig. 7).

3.2.1. Boundary conditions

(1) Inlet boundary

The inlet velocity at the entrance of the catalytic converter is assumed to be uniform and flows along the symmetrical axis of the converter. Here the inlet velocity V_{in} is 21.2 m/s calculated from the above measurement of the mass flow, and the density $\rho_{g,in}$ is assumed to be 1.0 kg/m^3 before time 30 s and 0.8 kg/m^3 after time 30 s for simplicity. The inlet mass fractions of the species are supposed as follows: $c_{COg} = 0.0048$ mol/mol, $c_{O_2g} = 0.0048$ mol/mol, $c_{C_3H_6g} = 0.00065$ mol/mol. The turbulent kinetic energy κ is assumed to be 0.02 m^2/s^2 and its dissipation rate $\varepsilon = 0.01$ m^2/s^3. The inlet temperature changes as shown in Fig. 8.

(2) Outlet boundary

The outlet boundary condition is treated as a fully developed flow, namely the gradients of all variables (except pressure) are zero. The outlet mass flux must satisfy the mass conservation.

(3) Wall boundary

Wall boundary conditions in the free stream region are no-slip velocity boundary and adiabatic temperature boundary. The inlet and outlet ends of the monolith are also treated as an adiabatic temperature boundary.

3.2.2. Initial conditions

In the whole region of the catalytic converter, the initial velocity and concentrations of O_2, CO, C_3H_6 are set to be zero and the temperature is assumed to be 400 K.

3.3. Simulation results and analysis

3.3.1. Warm-up characteristics of the catalytic converter

Fig. 9(a)–(f) shows the temperature contours in the catalytic converter with a 40° cone angle at different time. The upper part of the figures illustrates the distribution of the monolith temperature T_s and the down part is the distribution of the gas temperature T_g (the flow direction is from left to right). From the figure we can see that the inlet temperature of the monolith is only 500 K at 10 s and the catalyst is not activated. At this time the temperature behind the monolith maintains the initial temperature of 400 K. At 20 s the inlet temperature of the monolith rises to 600 K and the catalyst is lighted off. Then the temperature in the front part of the monolith increases quickly and the gas temperature behind the monolith also begins to rise gradually. After 40 s the temperature changing trend becomes slow. At 60 s the gas temperature behind the monolith is close to the inlet temperature. At 80 s, the temperature behind the monolith greatly exceeds the inlet temperature and the highest temperature reaches 755 K. Meanwhile, the temperature in the whole region of the catalytic converter gradually tends to be

stable. At 100 s all of the temperatures are nearly uniform and stable. The highest temperature is up to 813 K.

From the above analysis of the warm-up behavior in the catalytic converter, it can be concluded that the monolith explores a series of heating processes by inlet gas flow and chemical reactions. The temperature difference in the monolith changes from a small value at the beginning to a large one and again to a small one at the end.

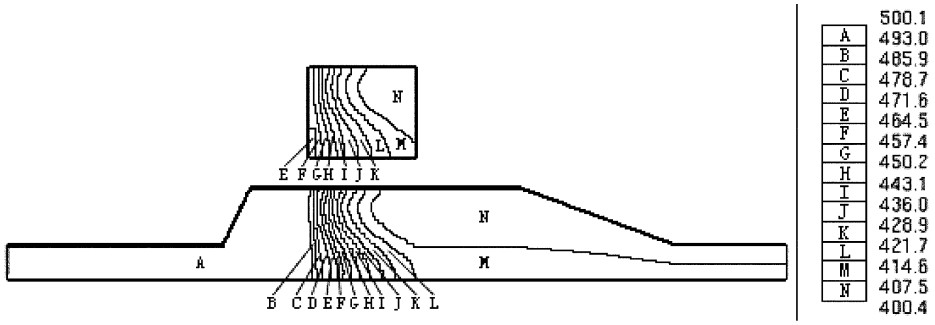

(a) 10 second

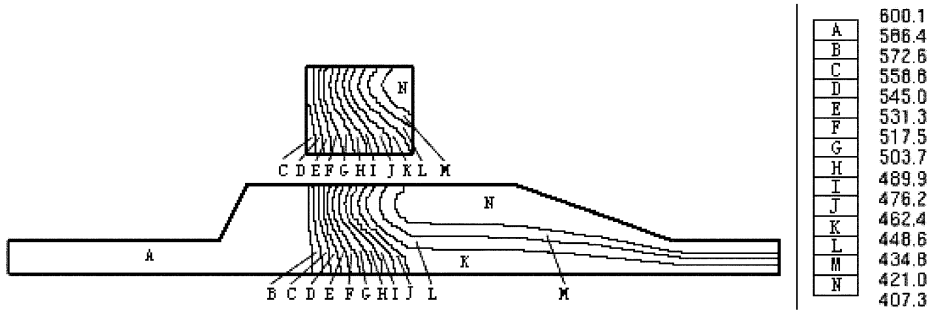

(b) 20 second

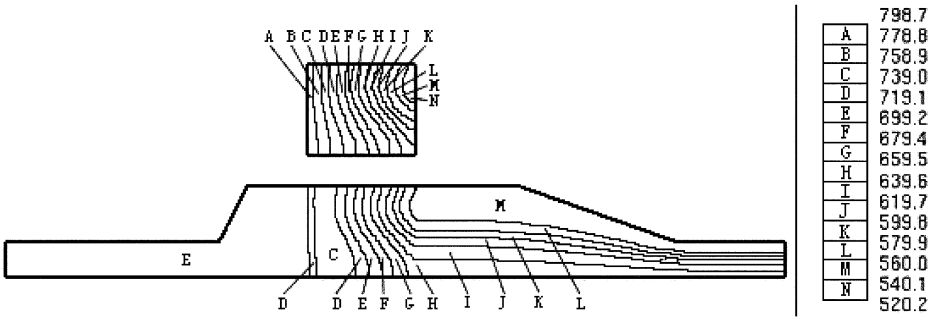

(c) 40 second

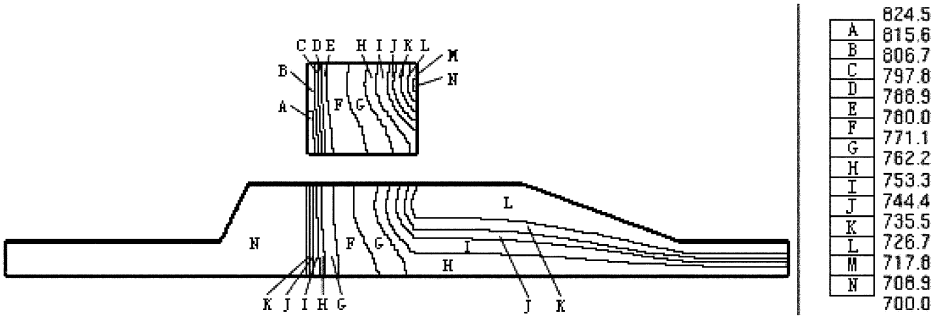

(d) 60 second

Fig. 10. Temperature contours of 120° catalytic converter at different time (K).

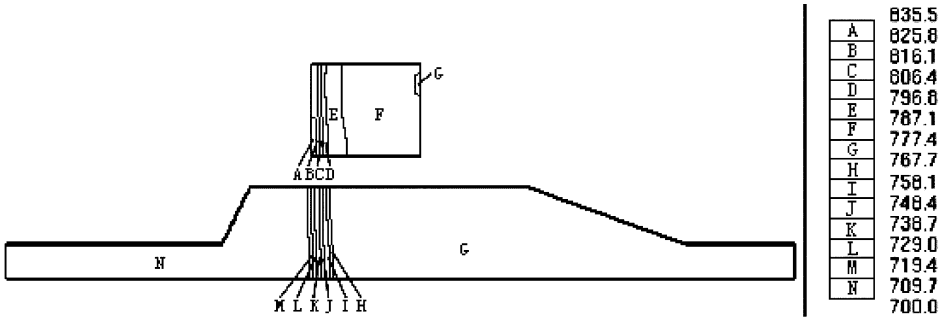

Fig. 10. (*Continued*).

In order to obtain the robust simulation, we need not only the correct mathematical description of the physical phenomena happened in the converter but also the reliable initial and boundary conditions for the converter. Here, due to the test limits and commercial CFD modeling limits, the initial and boundary conditions are not fully identical and consistent, and some assumptions are made to the property parameters. The simulation results are not directly compared with the measurements. However, the computed light-off behavior (see also Figs. 13 and 14) of the monolith has a qualitative agreement with the test results (see also Fig. 5 point 1). And the established model in this paper can essentially display the features of the flow, heat and mass transfer and chemical reactions occurred in catalytic converters.

3.3.2. Effect of inlet cone structure on warm-up characteristics

In order to investigate the effect of the inlet cone structure on the temperature distribution, the flow including heat and mass transfer and chemical reactions in the catalytic converter with a 120° cone angle is also simulated. Compared with the 40° catalytic converter, the 120° catalytic converter has the same computational conditions except for a different cone angle.

Fig. 10(a)–(f) shows the temperature contours in the catalytic converter with a 120° cone angle at different time. From the comparison between Figs. 9 and 10 it is found that there are some differences existed in the temperature distribution and warm-up behavior between two converters although they have a similar temperature change trend. For the 120° catalytic converter the catalyst is not lighted off at 10 s. In this case two catalytic converters have no obvious differences for the temperature distribution along axial direction, but the 40° catalytic converter has a more uniform temperature distribution along radial direction.

Fig. 11 shows the comparison of the temperature distribution along radial direction in the middle sections (at $x = 0.5L$) of the monoliths at 10 s. From the figure it can be

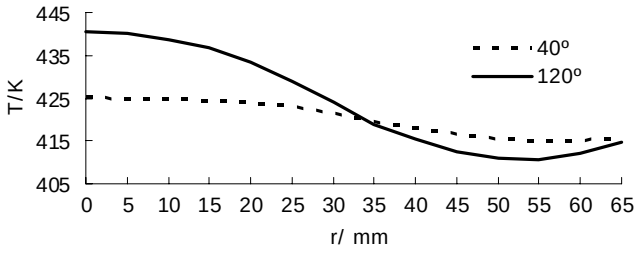

Fig. 11. Temperature distribution at $x = 0.5L$.

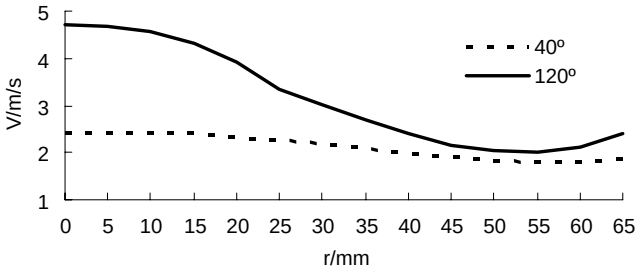

Fig. 12. Axial velocity distribution at $x = 0.5L$.

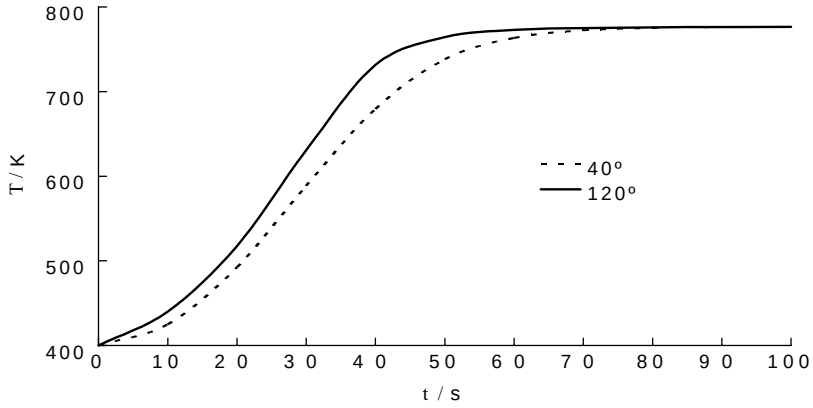

Fig. 13. Warm-up characteristics at $r = 0$, $x = 0.5L$.

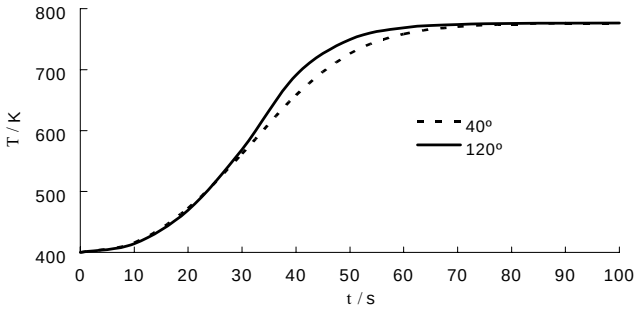

Fig. 14. Warm-up characteristics at $r = R$, $x = 0.5L$.

seen that for the 120° catalytic converter the temperature difference between the center and the edge in the monolith is about 30 K, but for the 40° catalytic converter it is less than 10 K. This temperature distribution is consistent with the velocity distribution in the same location at the same time, as shown in Fig. 12, which means that the gas velocity has a significant influence on the temperature distribution in catalytic converters.

Figs. 13 and 14 show the warm-up behaviors at the center and at the edge in the middle section of the monoliths, respectively. From these figures we can clearly see that the temperature of 120° converter exceeds the temperature of 40° converter as time goes on, and the largest temperature difference is more than 50 K at about 40 s. However, as the temperature tends to be stable, the difference becomes smaller and smaller. In addition, the difference is larger at the center than at the edge. This is because the flow velocity at the center of 120° converter is higher than that of the 40° converter (see also Fig. 12) and the inlet temperature can quickly conduct into the monolith, which results in a rapid light-off of the catalysts. Moreover, the heat released from chemical reactions accelerates the warm-up of the monolith.

4. Conclusion

From the experiment and numerical simulation of the temperature fields of the catalytic converters, the conclusions can be drawn as follows.

(1) Heat convective transfer between the exhaust gas and the monolith, heat conduction in the monolith, heat from chemical reactions, and flow velocity distribution are all main factors affecting the temperature distribution and warm-up characteristics.
(2) For catalytic monolith, when the catalyst is not activated, the temperature distribution and warm-up characteristics of the monolith are similar to uncoated-monolith. However, after the catalyst is activated, the high temperature appears in the rear center part of the monolith.
(3) A multi-dimensional flow including heat and mass transfer, chemical reactions is numerically simulated. Although the model contains many simplifications and assumptions it has been demonstrated that it can predict the warm-up behavior of the catalytic converter and the effect of the inlet cone structure on the warm-up behavior.
(4) Simulation results show that the 120° catalytic converter has a better light-off performance than the 40° catalytic converter, especially in the center of the monolith.
(5) Further study includes quantitative validation of the model, the modeling of more than two reacting species, external heat loss and the thermal inertia effects of the catalyst matting and can.

Acknowledgements

This research is supported by National Natural Science Foundation of China, Grant No. 50076021.

References

[1] J.R. Mondt, Cleaner Cars: The History and Technology of Emission Control Since the 1960s, Society of Automotive Engineers Inc., Warrendale, PA, 2000.
[2] G. Glander, S. Zidat, Modeling electrically heated converters, Automotive Eng. Int. (2) (1998) 76–78.

[3] S.J. Shuai, J.X. Wang, R.J. Zhuang, J.R. Chen, Study on flow characteristics of automotive catalytic converters with various configurations, SAE Paper 2000-01-0208.
[4] D.K.S. Chen, E.J. Bissett, S.H. Oh, A three-dimensional model for the analysis of transient thermal and conversion characteristics of monolithic catalytic converters, SAE Paper 880282.
[5] K. Zygourakis, Transient operation of monolith catalytic converter: a two-dimensional reactor model and the effects of radially nonuniform flow distributions, Chem. Eng. Sci. 44 (1989) 2075–2086.
[6] R.J. Clarkson, S.F. Benjamin, T.S. Jasper, N.S. Girgis, An integrated computational model for the optimization of monolith catalytic converters, SAE Paper 931071.
[7] R.I. Issa, Solution of the implicitly discretized fluid flow equation by operator splitting, J. Comput. Phys. 62 (1986) 40–65.